IMPROVEMENT OF TOE RESISTANCE OF DRILLED SHAFT FOUNDATIONS IN HIGHLY VARIABLE SEDIMENTARY SOILS USING SMART CELLS

Antonio Marinucci, PhD, MBA, PE, Advanced Foundation Solutions LLC; New York, N.Y., USA, E-mail: AMarinucci@AdvFoundations.com
Mario A Terceros Herrera, Incotec S.A., Santa Cruz de la Sierra, Bolivia, math@incotec.cc
Mario Terceros Arce, Incotec S.A., Santa Cruz de la Sierra, Bolivia, mta@incotec.cc

ABSTRACT: A Smart Cell is a closed-type tip post-grouting device that is attached to the bottom of the steel reinforcement cage of a drilled shaft and is used to enhance performance and to reduce uncertainty thereof. Control of the grout is maintained within the device during injection and a uniform stress is imparted across entire base area simultaneously, inducing a pre-mobilization load into the shaft as well as the soil. This paper describes the construction and tip post-grouting of drilled shafts from two bridge projects in the Santa Cruz, Bolivia region along the Paraí River. During the grouting process at each project site, there were noticeable differences in the grouting pressures achieved and responses observed, even within short distances between shafts. For this project, the greater benefit of using the Smart Cells was the reduction of risk and uncertainty of performance due to the highly variable soil conditions. Ultimately, since the response of each shaft was observed during grouting and because a "minimum" value of shaft resistance (i.e., pre-mobilization of load) was measured, there is a greater reliability with the anticipated performance of the shafts when axial loading is eventually applied.

Keywords: tip post-grouting, design, performance, risk, uncertainty

INTRODUCTION

Given the various concerns and uncertainty faced during design and construction, understanding load transfer in side and tip resistance and the factors that affect each component are essential to ensure the design is optimized and constructible as much as practical (or permissible). As an axial compressive load is applied to the top of a drilled shaft, the shaft moves downward relative to the in-situ soil, where the axial resistance afforded by the soil is first mobilized in side resistance and then in end resistance. The generalized load transfer behavior of an axially compression loaded conventional, ungrouted drilled shaft is presented in Figure 1a. The side resistance will mobilize its peak strength after a minimal amount of vertical displacement, approximately equal to about 0.2% to 0.4% of the diameter of the shaft (i.e., normalized displacement), regardless of soil type. At this vertical displacement, the end resistance that has mobilized is relatively small. The end resistance does not fully mobilize until much larger displacements have been realized, approximately equal to about 4% to 5% of the shaft diameter in cohesive soils and about 10% in cohesionless soils. As such, due to this strain incompatibility in achieving the peak strength, designers neglect either side or end resistances or discount or reduce their relative contributions.

Tip post-grouting is a technique used to inject a neat cement grout under pressure beneath the base of a drilled shaft to enhance or improve the axial load-displacement performance of the shaft (compared to a conventional, ungrouted pile) by improving the mobilization of side and end resistances, increasing the axial resistance of the pile, and better aligning the load transfer curves (Figure 1b). During injection, a bi-directional force is induced by the pressurized grout to the drilled shaft and to the soil below, which results in a pre-mobilization (i.e., preloading) of the side and end resistances. The downward force into the soil below the base of the shaft enhances the stiffness in the load-displacement response (at intermediate loads) and results in better alignment with the side resistance load transfer response. In essence, the greater amount of load that can be induced from the injection process, the greater amount of pre-mobilization and improvement in performance that can be achieved (Loehr et al, 2017).

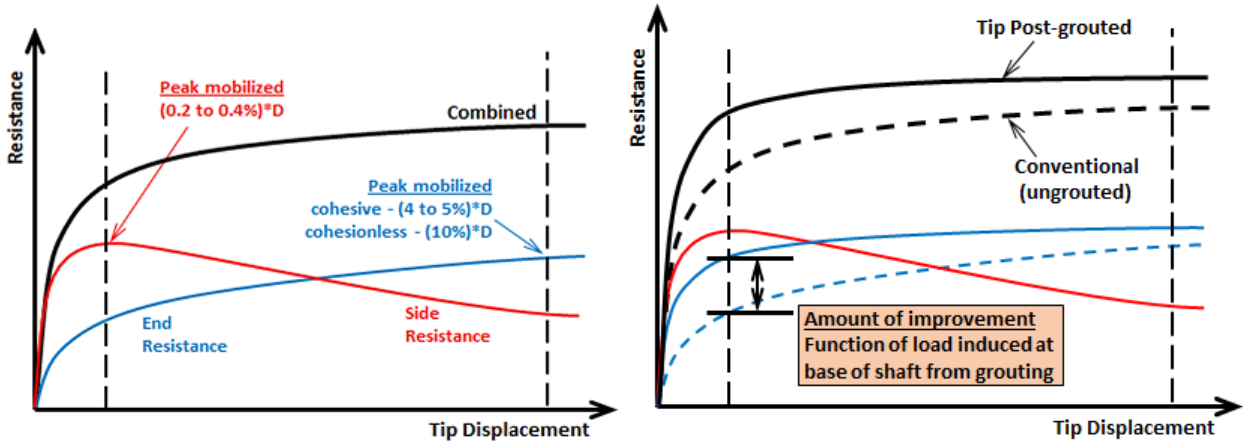

Figure 1. Generalized load transfer behavior: (a) conventional, ungrouted drilled shaft (mod. from Brown et al., 2010) and (b) tip post-grouted drilled shaft

SMART CELLS – OVERVIEW AND QUALITY CONTROL

A Smart Cell (SC) is a closed-type tip post-grouting device that is attached to the bottom of the steel reinforcement cage of drilled shafts and acts, essentially, as a piston-cylinder system (i.e., a hydraulic jack). The diameter of the SC is smaller than the overall diameter of the drilled shaft to ensure the device and cage can be installed to the desired depth, to prevent scraping of the sidewall of the borehole during installation, and to prevent inducing any surcharge pressures as the assembly is placed to the bottom of the hole. Photographs of the SC after fabrication and attached to the bottom of the steel reinforcement cage are presented in Figure 2, where the non-woven geotextile (Figure 2b) is used to act as a filter containing the grout when/if any leakage through the device may occur.

Figure 2. Photographs of the Smart Cell (a) after fabrication but prior to installation and (b) attached to the bottom of the steel reinforcement cage

The SC is a relatively rigid system where the internal and outside dimensions of the device are known. The amount of bi-directional load induced can be computed in a very straightforward manner: induced load (P_{SC}) = injection pressure (p) x cross-sectional area of the device (A_{SC}). In addition, the pressure acts across the entire base of the device simultaneously. This type of device can be used in any type of ground condition, as the grout is contained within the device itself, reducing or eliminating the concern and potential of hydrofracture. The access tubes for nondestructive integrity testing (NDT) and/or hollow bar steel reinforcement bars can be integrated into the tip post-grouting device to serve as the access tubes for NDT and to deliver the grout to the device, while eliminating congestion within the reinforcement cage.

The general procedure used when tip post-grouting is performed is described below in the following paragraphs. The borehole is drilled using conventional drilling techniques (i.e., dry method, wet method, and/or casing method). Then, the steel reinforcement cage with appropriate appurtenances (e.g., NDT

access tubes, instrumentation, SC device, and components) is installed in the borehole, which is then filled with concrete and allowed to cure (Figure 3a). The required NDT is performed at the appropriate time depending on the NDT method used and the hydration process/compressive strength of the concrete.

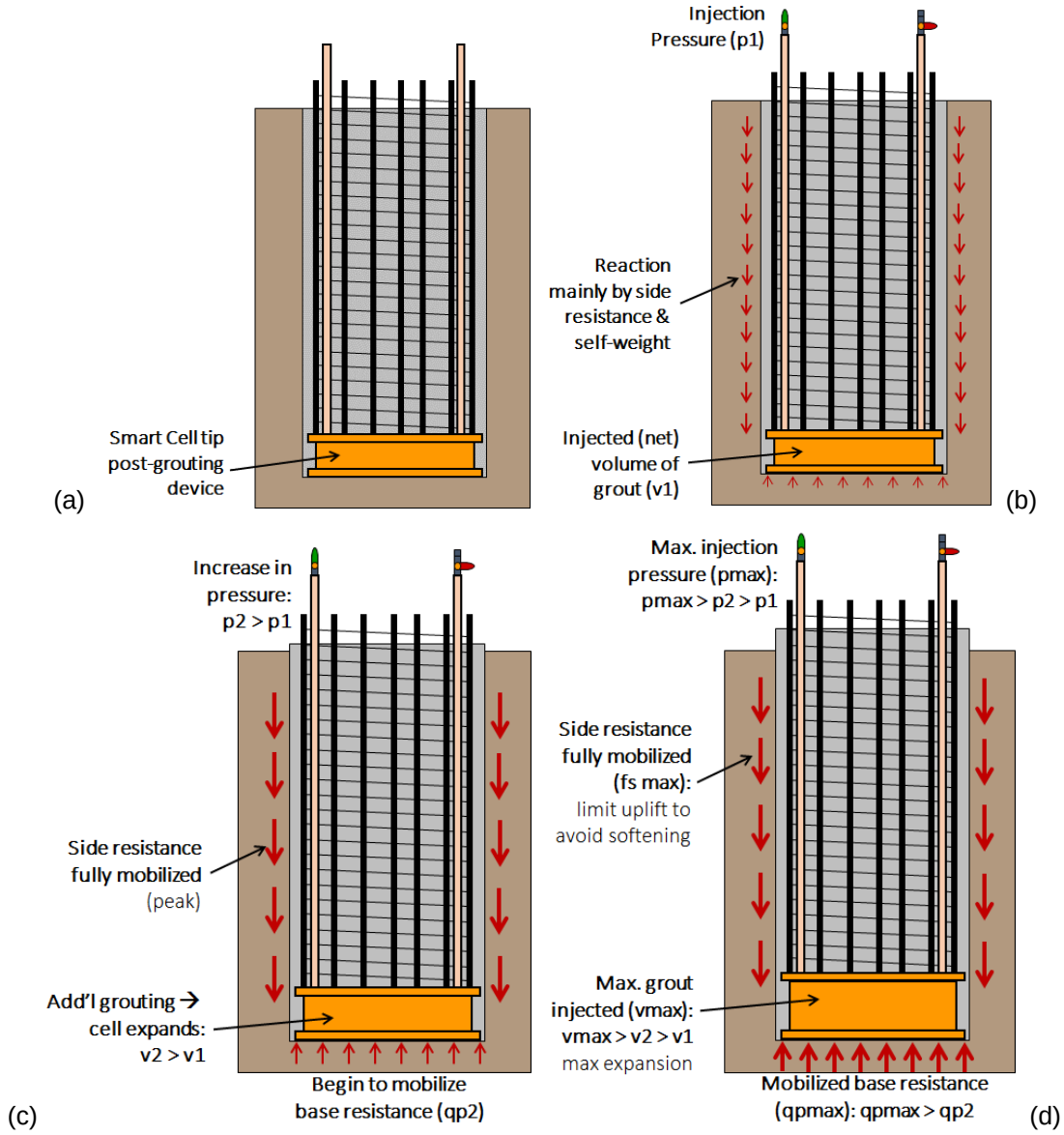

Figure 3. Generalized sequence: (a) installation into borehole and concrete placement, (b) commencement of grouting, (c) intermediate grouting stages, and (d) grouting completed

After the concrete has achieved the minimum required unconfined compressive strength (f_c'), the tip post-grouting operation can be performed, whereby grout is injected under pressure into the SC. Typically, a neat cement grout (i.e., no aggregate) with a water-to-cement ratio (w/c) between 0.45 and 0.55 is used for tip post-grouting. The injection pressure and, therefore, the induced bi-directional load that can be applied to the shaft and the soil is a function of the in-situ stress state of the soil, self-weight of shaft, and available side resistance between the shaft and the surrounding soil. During grout injection, negative side resistance and positive end resistance in the soil are induced (Figure 3b). During the early stages of this process, the side resistance begins to mobilize and the contribution from the end resistance is minimal (Figure 1). At some instant during the intermediate grouting stages, the side resistance is fully mobilized (peak strength)

and the end resistance is beginning to mobilize as a result of the preloading and stiffening effect from the tip post-grouting (Figure 3c). The tip post-grouting is continued until the prescribed grouting criteria (i.e., uplift displacement, volume injected, grout pressure, and/or expansion limit of the SC device) is achieved (Figure 3d). At that point, ideally, the end resistance will have been fully mobilized under the grouting conditions while the side resistance would not have been degraded to a strain-softened state.

The grouting is performed using a controlled process to ensure proper performance of the system and the shaft as well as to ensure that minimal-to-no generation of excess pore water pressure occurs. The injection pressure, volume and flow of grout, and movements at the top of the shaft and at the SC device are measured and recorded throughout the grouting operation (Figure 4). The injection pressure is typically measured at the top of the shaft immediately before the grout enters the embedded grout tube and may also be measured at the grout mixer. Upward displacement of the drilled shaft is measured using dial gauges and/or LVDTs mounted on an independent frame and/or by using digital survey or other optical survey means. The expansion of the cell is typically measured using telltales mounted to the bottom and/or top of the SC device to provide a quantitative understanding of the movement of the SC (i.e., amount of expansion and direction of the relative movements). The volume of grout injected into the SC can be measured using a flow meter (most common), counting of the strokes of the pump, and/or by summating the net amount of grout mixed (via bags of cement and water used). Throughout the process, real-time or near real-time plots of grout pressure vs. injected volume, grout pressure vs. shaft uplift, and grout volume vs. shaft uplift are monitored for conformance with the grout criteria.

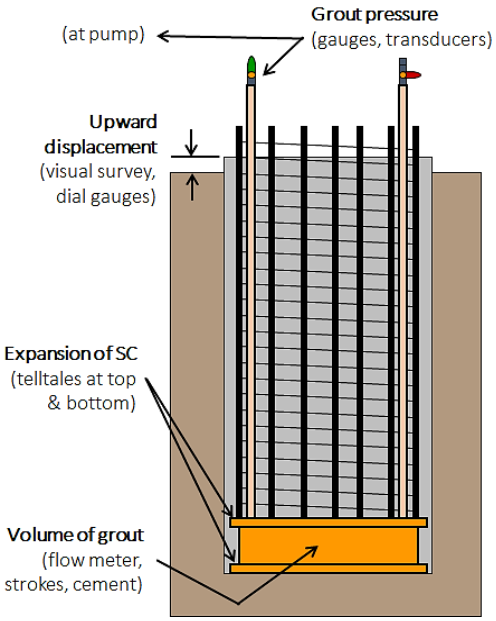

Figure 4. Monitoring locations of the QC program during grouting

During the post-processing and analysis of the results, additional graphs are constructed to enhance the understanding of the behavior from the tip post-grouting operation. A plot of the induced load (P_{SC}) vs. measured displacement (bottom of the SC) provides valuable insight into the behavior of the shaft and the soil during the grouting process. As an example, as shown in Figure 5a (where: red line = shaft uplift; blue line = downward movement), there was a recompression of soft/loose or disturbed soil at the bottom of the shaft during the early/intermediate stages of the grouting (i.e., up to about 1,000 kN of induced load), after which there was a compression of the soil resulting in an increase in soil stiffness and a premobilization of the load into the soil and shaft. This behavior corresponds to the measured uplift displacement of the shaft, for which no movement was realized until after the soft bottom was restored and the soil compressed (i.e., after an induced load of about 1,800 kN). If there had been minimal to no soft/loose or disturbed soil at the bottom of the shaft, the slope of the curve of downward movement would have been flatter without the initial steep slope (i.e., higher soil stiffness).

Graphing the injection pressure vs. grout volume provides the benefit of qualitative indication of soil type present at the base of the drilled shaft. Based on experience with performing multiple tip post-grouting operations in various soil conditions, the shape and trend of the pressure vs. volume curve provides evidence whether the soil type is cohesionless or cohesive. As an example, as shown in Figure 5b, the two curves (C6N3 and C9N3) represent the tip post-grouting response of two piles located about 400 ft (120 m) from each other along the alignment for the same bridge project. These piles were both 5 ft (1500 mm) in diameter and installed to a depth of about 70 ft (21.5 m) using the casing method. Tip post-grouting was performed

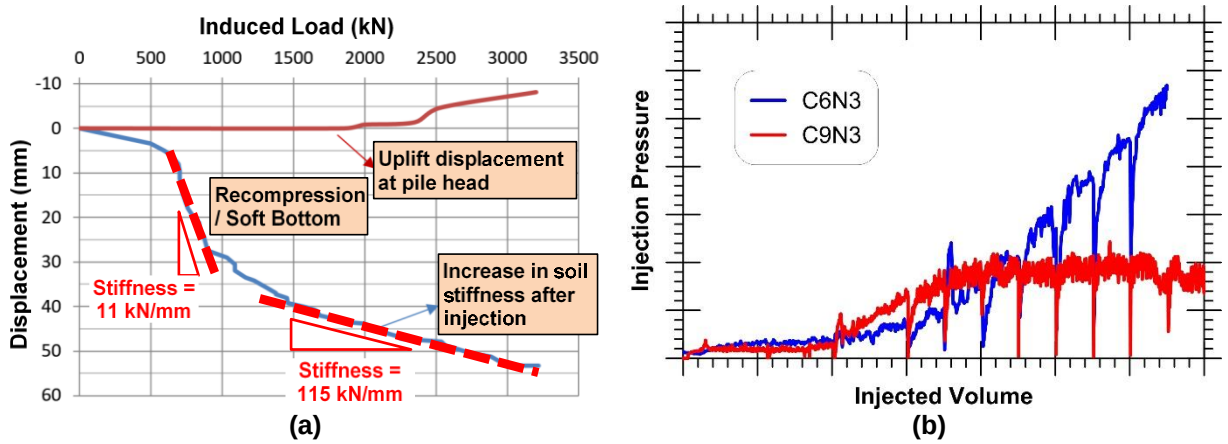

Figure 5. Examples of grouting data: (a) induced load vs. uplift/downward displacement (indicating soil stiffness at base) and (b) injection pressure vs. grout volume (indicating soil type)

in a similar manner for both piles (the spikes represent planned pauses in the grouting operation to perform manual measurements and to limit the develop of excess pore water pressure).

There is a noticeable difference in the grouting record for the two piles in Figure 5b. C6N3 was embedded into a dense sandy soil (fines content, FC=13%), whereas C9N3 was tipped into a high plasticity clay (FC=93%). The pressure vs. volume relationship presented in Figure 5b is similar in nature to the normalized load-displacement curve of a drilled shaft in axial compression in cohesive and cohesionless soils (Chen and Kulhawy, 2002), as shown in Figure 6. C9N3 exhibited a relatively low final grouting pressure (compared to expected) and no further increase in pressure occurred for continued pumping of grout as the end bearing of the shaft was fully mobilized and likely failed, which has been observed for tip post-grouting in cohesive soils. However, the pressure for C6N3 continued to increase with continued grouting, and the grouting eventually was terminated when the side resistance was exceeded, and the excess uplift was observed.

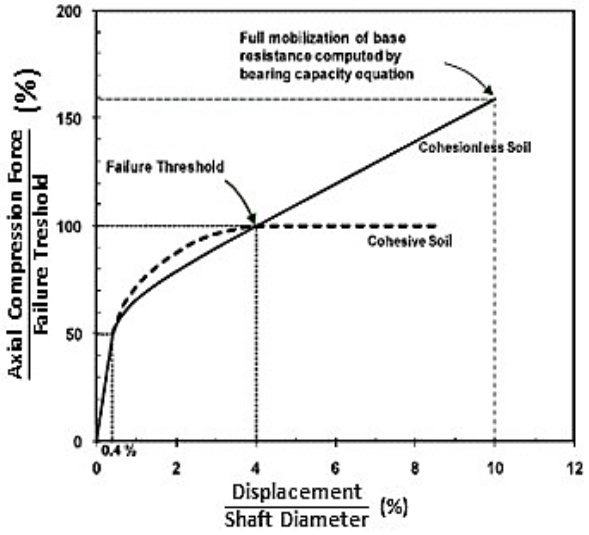

Figure 6. Normalized load-displacement curve of a drilled shaft in axial compression in cohesive and cohesionless soils (Chen and Kulhawy, 2002)

DESIGN CONSIDERATIONS – TARGET PRESSURE

For tip post-grouting with a SC device, the load-displacement curve presented by Chen and Kulhawy (as described in Brown et al, 2018) is used to compute the target injection pressure based on the prescribed tolerable displacement of the drilled shaft. The amount of allowable vertical displacement when the structure is loaded (i.e., performance criteria) indirectly establishes the amount of axial resistance that can be mobilized for that given displacement (service conditions). If the allowable displacement is less than that required to fully mobilize the axial resistances, tip post-grouting can be used to induce a bi-directional force to pre-mobilize the required axial resistance. As discussed above, the side resistance is fully mobilized at a normalized displacement of about 0.2% to 0.4%, while the end resistance is mobilized at a normalized displacement of about 4% to 5% for cohesive soils and about 10% for cohesionless soils. A graphical representation of the normalized load-displacement relationship of a drilled shaft in axial compression in cohesive and cohesionless soils is presented in Figure 6. The vertical axis represents the ratio of axial

compression load to the failure threshold, which is defined as the nominal resistance. As shown on the figure, 100% of failure threshold typically occurs at a normalized displacement of about 4% for both soil types. For drilled shafts bearing in cohesive soils, the axial compression force is maximum once the failure threshold is reached, whereas in cohesionless soils, the axial compression force increases (i.e., increasing end resistance) from a normalized displacement of 4% to 10%, when the maximum axial compression force (i.e., fully mobilized end resistance) is achieved.

The general procedure used to estimate the required target pressure (and the induced load, P_{SC}) is described below in the following paragraphs. The drilled shaft must be designed to satisfy service, strength, and extreme event limit state conditions. The geotechnical engineer designs the drilled shaft (i.e., diameter and depth) to resist the anticipated imposed loading while satisfying the applicable limit state conditions. Once the diameter and depth of the drilled shaft have been established using the appropriate axial end and side resistances provided by the in-situ ground conditions (strength limit state), the estimation of target pressure for pre-mobilization can be performed (service limit state conditions).

A hypothetical example will be used to convey the premise of the design approach. Assume a 6 ft (1.8 m) diameter drilled shaft is installed to an embedment depth of about 98 ft (30 m) into a heterogeneous soil deposit consisting of sandy soils overlying clayey soils. The structural engineer provided that the service design loading was about 905 kips (4030 kN) and no more than about 1 in (25 mm) of vertical displacement of the top of the drilled shaft could be tolerated. Based on the geotechnical report, the nominal side and end resistances were estimated to be about 265 kip (1180 kN) and 450 kip (2000 kN), respectively. The self-weight of the shaft was estimated to be about 200 kip (890 kN). For a normalized displacement of 1.4% (1 in/72 in), approximately 70% of the axial compressive force (i.e., the design load plus the self-weight of the shaft) would be mobilized at the maximum allowable displacement (from Figure 6). For a total nominal resistance of 715 kip (3180 kN), the mobilized axial compressive force is computed as 70% multiplied by the nominal resistance to equal about 500 kip (2224 kN). The service resistance force is then computed as the axial compressive force less the self-weight of the shaft and is equal to about 300 kip (1335 kN). For the purposes of this example, assume that the outside diameter of the plates of the SC is 62 in (1575 mm) resulting in a bearing area of about 21 sq ft (1.95 sq m); in addition, the internal diameter within the SC is 59 in (1499 mm) resulting in a cross-sectional area of about 19.0 sq ft (1.77 sq m). The target injection pressure is then computed as the design load less the service resistance force divided by the internal area of the SC device. For this example, the target injection pressure would be equal to about 220 psi (10.6 kPa).

MINI PROJECT CASE HISTORIES

The construction, tip post-grouting, select results, and general observations from the grouting performed on the more than 70 total drilled shafts for a railway bridge and a vehicular bridge in the Santa Cruz, Bolivia region along the Paraí River will be presented and discussed below. The conditions in the Paraí River can vary drastically throughout the year from near dry/very low water level to near flood stage levels. The general subsurface conditions consist of highly variable soil deposits, bedding, composition, and characteristics, which are understandable and expected given that the site is located within a dynamic river environment, where it is common to find subsurface paleo channels containing highly variable soil conditions. Using the procedure described previously, the target pressure for the tip post-grouting at each bridge location was computed for its worst-case condition. As discussed above, the injection pressures that can be achieved are directly dependent upon the in-situ soil conditions, available end and side resistance, and the self-weight of the drilled shaft.

The drilled shafts were constructed using temporary segmental casing without the use of a drilling support fluid. A SC device was attached to the bottom of the steel reinforcement cage (along with the grout tubes and instrumentation) and lowered into the borehole, after which the concrete was placed the using tremie method. The outside diameter and pre-injection height of the SC device were about 37.5 inches (95 cm) and 12.3 inches (31 cm), respectively. After the concrete in the drilled shaft achieved a minimum

unconfined compressive strength of about 1,450 psi (10 MPa) and/or when the water level within the river permitted work to proceed, the tip post-grouting was performed individually for each drilled shaft. Monitoring and recording of injection pressure, grout volume injected, and grout flow rate were performed in real time using transducers connected to a data acquisition system and observed on a laptop computer. The uplift and downward movements of the drilled shaft and the SC were measured using manual readings obtained via visual survey and tell-tales, respectively.

Foianini Bridge The new Foianini Bridge will be constructed adjacent to the existing bridge (Figure 7), which connects the municipalities of Porongo and Santa Cruz. The new bridge will be about 36 ft (11 m) wide and about 1,380 ft (420 m) in length. The 5-span bridge will be supported by four pier structures, located about 330 ft (100 m) apart and each with seven drilled shafts, located in the Paraí River and two abutments supported by 3 drilled shafts each, which are located beyond the extents of the river's edges.

Figure 7. View of drilled shafts being constructed for new bridge adjacent to existing Foianini Bridge.

At the center of each of the four pier locations, one soil boring was performed to a depth of about 130 ft (40 m) along with Standard Penetration Testing (SPT). The soil deposit is classified as quaternary sedimentary silty-clayey sands of alluvial and flood plain origin (Chaco–Beniana Plain of the Amazonian Plains), with thicknesses that exceed 165 ft (50 m) in some areas. The general subsurface profile (Table 1) contains an upper layer of granular fill underlain by highly heterogeneous and interbedded layers consisting of lean to highly plastic clay, clayey silt to sandy silt, and fine to gravelly sand with clay and silt, with gravel (east side of alignment) located at depths beginning around 125 ft (38 m). The drilled shafts were tipped into clayey sand (west abutment and pier 2), clay (pier 3), sandy silt (pier 4), and silty clay (pier 5 and east abutment).

Table 1. Subsurface profile at Foianini Bridge

PD-01 at Pier 2 (in ft)			PD-02 at Pier 3 (in ft)			PD-03 at Pier 4 (in ft)			PD-04 at Pier 5 (in ft)		
Top	Bottom	Description	Top	Bottom	Description	Top	Bottom	Description	Top	Bottom	Description
0.0	8.2	Granular fill	0.00	9.84	Granular fill	0.0	8.2	Granular fill	0.0	8.2	Granular fill
8.2	9.8	Clay	9.84	19.68	Clay w sand	8.2	13.1	Sand	8.2	27.9	Clayey silt
9.8	13.9	Silt w sand	19.68	26.24	Sandy silt	13.1	37.7	Clay w sand	27.9	32.8	Sand
13.9	38.0	Clay w sand	26.24	45.92	Clay w sand	37.7	42.6	Sand w silt	32.8	37.7	Clay
38.0	46.7	Sand w silt	45.92	55.76	Silty sand	42.6	67.2	Clay w silt	37.7	42.6	Sand
46.7	54.1	Clay	55.76	85.28	Sand w silt	67.2	77.1	Sand w gravel	42.6	57.4	Silty clay
54.1	75.4	Sand w silt	85.28	92.82	Silty sand	77.1	82.0	Sand w silt	57.4	67.2	Sand
75.4	100.7	Clayey sand	92.82	117.10	Clay w sand	82.0	85.3	Clay	67.2	82.0	Silty clay
100.7	119.7	Sandy clay	117.10	131.20	Sand w silt	85.3	91.8	Sand w gravel	82.0	86.9	Silty sand
119.7	131.2	Sand w silt				91.8	116.4	Sandy silt	86.9	91.8	Clay
						116.4	126.3	Clayey silt	91.8	96.8	Silty sand
						126.3	131.2	Silty sand	96.8	121.4	Silty clay
									121.4	131.2	Sand to rock

The bridge superstructures and substructures were designed in general accordance with the AASHTO LRFD Bridge Design Specifications (2012). Each of the drilled shafts was 4 ft (1200 mm) in diameter with an embedment depth of about 98 ft (30 m). At this location, the design scour depth for structures within the river was specified as 46 ft (14 m). The service load per drilled shaft was specified as 882 kip (4027 kN) with a maximum allowable vertical settlement of 1.2 in (30 mm). For an allowable displacement of 1.2 in

(30 mm) and a service load of 882 kip (4027 kN), the minimum required target pressure was estimated to be about 150 psi (10.3 bars).

As shown in Table 2 and Figure 8, there was considerable variability in the observed behavior and measured responses from the tip post-grouting operation. There were notable differences in injection pressures achieved for the various shafts at the bridge structure, even within short distances at the same pier or abutment structure. Considering the general behavior, the normalized uplift and normalized downward displacements ranged from 0% to 0.4% and from 1% to 8.8%, respectively, resulting in maximum unidirectional induced loads of 346 to 808 kip (1538 to 3595 kN). The unidirectional induced load ranged from about 40% to 92% of the design service load.

Table 2. Tip Post-grouting behavior at Foianini Bridge

	Max. Pressure psi [bar]	Max. Unidirectional Induced Load, kip [kN]	Max. Uplift inch [mm]	Max. Downward Displacement, inch [mm]
Range	138 to 500 [9.5 to 34.5]	346 to 808 [1538 to 3595]	0 to 0.2 [0 to 4]	0.5 to 4.2 [12 to 106]
Average	315 [21.7]	590 [2623]	0.1 [2.5]	1.8 [46.8]

The injection pressure vs. volume and the unidirectional induced load vs. displacement relationships from the grouting performed at Pier 4 for shafts 3 and 6 are presented in Figure 8. As can be seen, the differences in the grouting pressure being achieved varied considerably between the two shafts: maximum pressure of about 220 psi (15.2 bar) and 520 psi (35.8 bar) for shafts 4 and 6, respectively (Figure 8a). In addition, even the development of the pressure during injection was notably different: relatively flat for shaft 3 whereas there was a relatively steep increase in pressure during the early stages followed by a drop off in sustained pressure for shaft 6. From Figure 8b, the response, in general, of shaft 6 was notably stiffer than that of shaft 3, with the exception of toward the end of the grouting where the load-displacement curves were relatively parallel to each other. The stiffness response for both shafts decreased appreciably by a displacement of 0.5 in (13 mm). After a downward displacement of about 0.5 in (13 mm) of the SC into the underlying soil, there was a drastic increase in displacement for relatively small amount of gain in induced load, which seemed to stiffen after an additional displacement of 1.5 in (38 mm) possibly indicating a localized softer lens of soil within the influence zone of the loading.

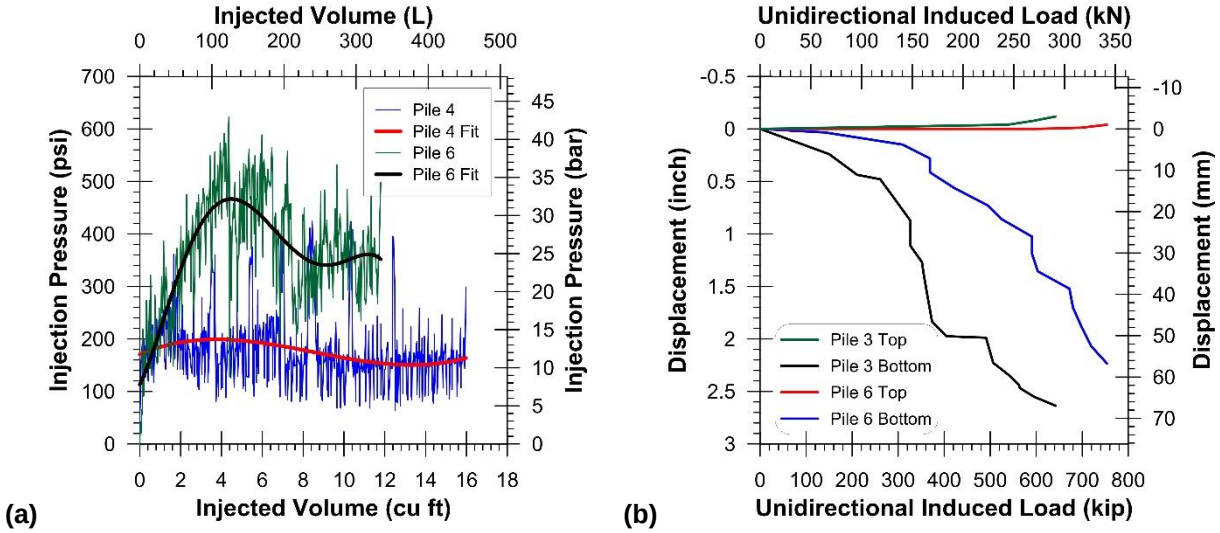

Figure 8. Results from tip post-grouting at Piles 3 and 6, Pier 4 at Foianini Bridge: (a) injection pressure vs. volume relationship and (b) unidirectional induced load vs. displacement

Railway Bridge The new 9-span Railway Bridge will be supported by eight pier structures, each with four shafts, and two abutments supported by four shafts each. The bridge will be about 33 ft (10 m) wide and about 1150 ft (351 m) in length. Due to the poor ground conditions of the near surface soils within the river, temporary earth berms/working platforms were required to construct the drilled shafts within the river's edges (Figure 9).

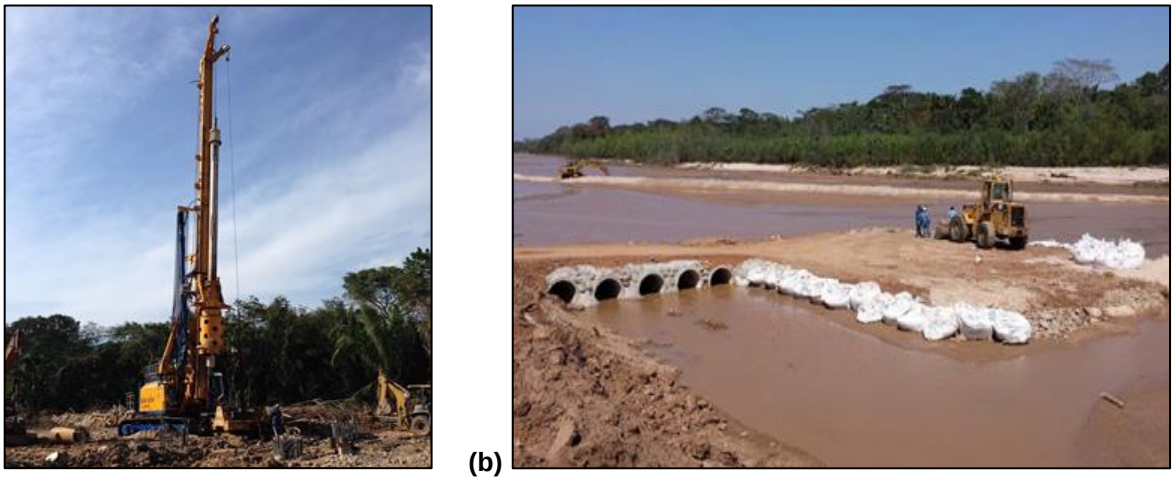

(a) (b)

Figure 9. Photographs of (a) construction of a drilled shaft at an abutment, and (b) installation of a working platform for drilled shaft construction in Piraí River for the new Railway Bridge

Two soil borings were performed to a depth of about 115 ft (35 m) along with Standard Penetration Testing (SPT). The soil deposit is highly heterogeneous with interbedded lenses and is classified as quaternary sedimentary silty-clayey sands of alluvial and flood plain origin (Chaco–Beniana Plain of the Amazonian Plains). The general subsurface profile (Table 3) contains an upper layer of loamy sand underlain by alternating layers of inorganic clay and silt, silty sand, and inorganic clay with localized lenses containing a wide range of soil particles from gravel to clay. The groundwater table dropped significantly from abutment to abutment, from a depth of about 5.3 ft (1.6 m) on the eastern side to a depth of about 26.3 ft (8 m) on the west. The drilled shafts were tipped into silty sand (west abutment), inorganic clay (piers 1 to 8), and silty sand (east abutment).

Table 3. Subsurface profile at Railway Bridge

Boring No. 1 (in ft)			Boring No. 2 (in ft)		
Top	Bottom	Description	Top	Bottom	Description
0	6.6	Loamy sand	0	5.2	Loamy sand
6.6	25.9	Inorganic clay & silt	5.2	18.0	Sand & silty sand
25.9	26.2	Silty sand	18.0	19.7	Inorganic clay
26.2	31.2	Inorganic clay	19.7	21.0	Sand lens
31.2	42.6	Silty sand	21.0	23.9	Inorganic clay
42.6	60.0	Inorganic clay	23.9	36.1	Sand & silty sand
60.0	61.7	Silty sand	36.1	45.9	Inorganic clay
61.7	63.3	Inorganic clay	45.9	58.1	Silty sand
63.3	83.6	Silty sand & sand	58.1	60.7	Loamy sand
83.6	84.6	Clay to gravel lens	60.7	72.2	Silty sand
84.6	91.2	Silty sand	72.2	73.1	Clay & sand lens
91.2	92.5	Clay to gravel lens	73.1	80.4	Silty sand
92.5	115.0	Inorganic silt & clay	80.4	115.0	Inorganic silt & clay

The bridge superstructures and substructures were designed in general accordance with AASHTO LRFD Bridge Design Specifications (2012). Each of the drilled shafts was 4 ft (1200 mm) in diameter with an embedment depth of about 82 ft (25 m). At this location, the design scour depth for structures within the river was specified as 33 ft (10 m). The service load per drilled shaft was specified as 1102 kip (4900 kN) with a maximum allowable vertical settlement of 1.2 in (30 mm). For an allowable displacement of 1.5 in (38 mm) and a service load of 1102 kip (4900 kN), the minimum required target pressure was estimated to be about 565 psi (39.0 bars).

As shown in Table 4 and Figure 10, there was considerable variability, in general, in the injection pressures achieved and the observed behavior from the tip post-grouting activities. However, it was interesting to observe similar general behaviors/trends between some of the drilled shafts that were tipped in different soil types (i.e., silty sand vs. inorganic clay), as shown in Figure 10, where dissimilar responses were expected. Considering the general behavior, the normalized uplift and normalized downward displacements ranged from 0% to 0.8% and from 1.7% to 7.3%, respectively, resulting in maximum unidirectional induced loads of 255 to 900 kip (1134 to 4004 kN). The unidirectional induced load ranged from about 23% to 82% of the design service load. Compared with the tip post-grouting performed at the Foianini Bridge, the average maximum pressure and average maximum unidirectional induced load achieved were slightly higher for slightly greater average uplift and downward displacements.

Table 4. Tip Post-grouting behavior at the Railway Bridge

	Max. Pressure psi [bar]	Max. Unidirectional Induced Load, kip [kN]	Max. Uplift inch [mm]	Max. Downward Displacement, inch [mm]
Range	154 to 765 [10.6 to 52.8]	255 to 900 [1134 to 4004]	0 to 0.4 [0 to 10]	0.8 to 3.5 [21 to 88]
Average	468 [32.3]	609 [2708]	0.1 [2.6]	2.0 [51.0]

The injection pressure vs. volume and the unidirectional induced load vs. displacement relationships from the grouting performed at Pier 5 for shaft 2 and at the West Abutment for shaft 1 are presented in Figure 10. Both shafts exhibited similar trends of response although shaft 2 at Pier 5 (S2P5) was tipped in inorganic clay and shaft 1 at the West Abutment (S1WA) was tipped in silty sand. The pressure vs. volume response (Figure 10a) for S1WA was similar to what was expected (i.e., continued increase in achieved pressure or induced load in the silty sand), but the response for S2P5 was contrary to what was anticipated (i.e., increased pressure achieved or induced load to a peak level followed by sustained or slightly decreased pressure for continued injection, as shown in Figures 5b and 6), although the magnitude of the pressures achieved were considerably greater for S1WA than for S2P5. As shown in Figure 10b, a smaller amount of downward displacement was required to achieve a given unidirectional induced load (e.g., 550 kip or about 250 kN), thereby indicating a softer condition at the base of S1WA than for S2P5. That is, there was a greater amount of recompression of the soil observed at S1WA (i.e., length of initial slope of load-displacement curve) than for S2P5 before the stiffness of the soil increase (i.e., flattening of the load-displacement curve).

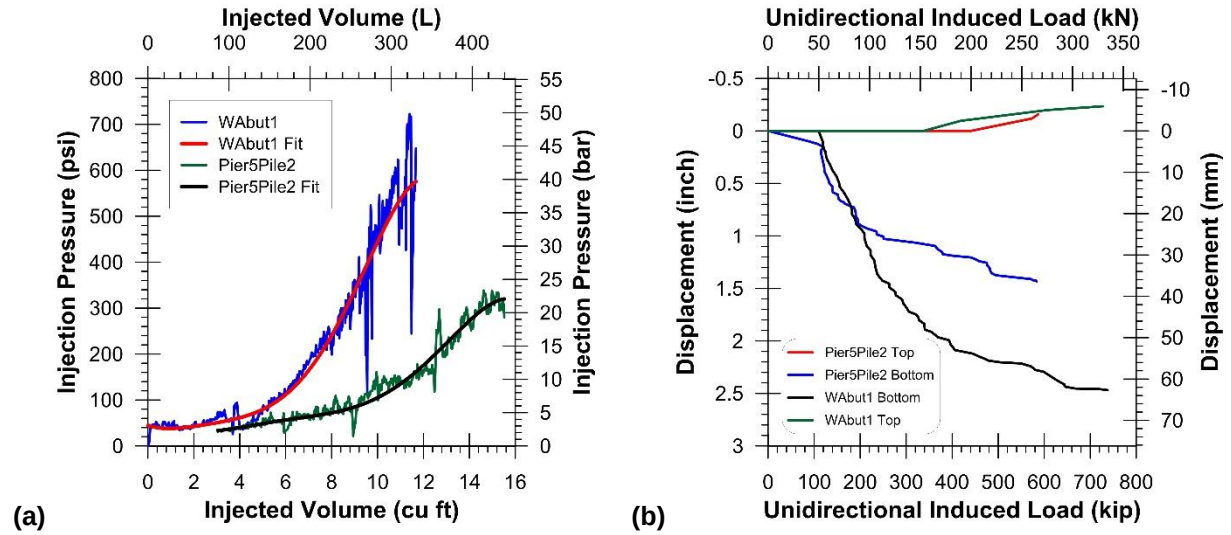

Figure 10. Results from tip post-grouting at Pile 2, Pier 5 and at Pile 1, West Abutment at the Railway Bridge: (a) injection pressure vs. volume relationship and (b) unidirectional induced load vs. displacement

CONCLUSIONS

An optimized maximum resistance cannot be realized by a conventional drilled shaft because full side resistance is achieved at very small vertical displacements, while full tip resistance is achieved at relatively large vertical displacements. Therefore, the objectives of implementing tip post-grouting are to enhance or improve the axial load-displacement performance of the drilled shaft via optimized alignment of the load transfer curves and/or by improved mobilization or preloading of shaft resistance. Successful and reliable implementation of tip post-grouting will allow designers to optimize the design of a tip post-grouted pile by stiffening its end-bearing response and by allowing the maximum tip resistance at a downward displacement that is consistent with the maximum side resistance (i.e., optimizing of load transfer curves). Cost efficient bored piles can be designed, which will lead to a reduction in the overall cost of, and greater reliability with, bored pile construction. Other benefits of tip post-grouting with a Smart Cell include stiffening the load-deformation response under working loads, reducing settlement of the pile under applied loading, shortened constructed length of the shaft, ability to be performed in a range of ground conditions, utilizing usable tip resistance in design computations, verifying a lower bound of axial resistance, and improving the ground beneath the base of the shaft. During grouting, loose soil or debris (i.e., soft bottom condition) is first compacted, and then, as the injection pressure increases, the in-situ soil is compressed, resulting in a pre-mobilization of end resistance.

This paper presented select results from tip post-grouting performed on more than 70 drilled shafts on for two bridge projects operation. For the grouting performed at both bridges, there was considerable variability in the injection pressures achieved and trends observed in the measured responses, even within short distances of adjacent or nearby drilled shafts. However, there were instances where the observed behavior or response was contrary to what had been observed on prior projects for a particular soil type. At the Railway Bridge, there were multiple instances where the observed pressure vs. volume relationship was similar for shafts tipped in silty sand as in inorganic clay but where a notable dissimilarity in behavior should have been realized. At the Foianini Bridge project, the unidirectional induced load ranged from 346 to 808 kip (1538 to 3595 kN), which equated to about 40% to 92% of the design service load. At the Railway Bridge project, the unidirectional induced load ranged from 255 to 900 kip (1134 to 4004 kN), which were approximately 23% to 82% of the design service load. Although differences in the responses of a drilled shaft under load, regardless of type of applied loading, is typically attributed to the effects of the construction technique and process employed, many of the differences at the two projects described herein can be explained by the highly variable depositional environment within the Paraí River, subsurface paleo channels, and the extreme heterogeneity of the alluvial soils containing highly variable soil conditions, composition, and characteristics.

REFERENCES

AASHTO. (2012). AASHTO LRFD Bridge Design Specifications, 6th edition. American Association of State Highway and Transportation Officials. Washington, D.C., 1661 pp.

Brown, D.A., Turner, J.P., Castelli, R.J., and Loehr, J.E. (2018). "Drilled Shafts: Construction Procedures and Design Methods." Geotechnical Engineering Circular No. 10. Report No. FHWA-NHI-18-024. Federal Highway Administration. March. 758 pp.

Chen, Y-J and Kulhawy, F.H. (2002). "Evaluation of Drained Axial Capacity for Drilled Shafts." Geotechnical Special Publication No. 116, Deep Foundations 2002, M.W. O'Neill and F.C. Townsend, eds., ASCE, Reston, VA, pp. 1200-1214.

Loehr, J.E., Marinucci, A., Hagerty Duffy, P., Gómez, J., Robinson, H., Day, T.J., Boeckmann, A.Z., and Cadden, A.W. (2017). *Evaluation and Guidance Development for Post-Grouted Drilled Shafts for Highways*, Report No. FHWA-HIF–17-024, Federal Highway Administration. March. 158 pp.

Marinucci, A. and Nichols, S.C. (2016). "Optimized Drilled Shaft Design through Post-Grouting," ASCE/Geo-Institute *GeoStrata* Magazine. May/June.